S-Band Aperture Efficiency of the DSS 13 26-Meter Antenna with the S-X Common Aperture Feed

M. J. Klein
Atmospheric Sciences Section

Measurements of the S-band performance of the DSS 13 26-meter antenna at Goldstone, equipped with the second-generation S–X common aperture feed, are reported. Aperture efficiency and overall antenna gain results are compared with predicted values. The elevation dependence of the aperture efficiency is reported.

I. Introduction

Precision measurements of astronomical radio sources have been analyzed to evaluate the gain and aperture efficiency of the 26-m antenna at DSS 13. The observations were made during January and February 1982 at 2270 MHz and 2295 MHz with the second generation S-X common aperture feed (Ref. 1), which was installed in November 1981. The results have been used to compare the performance of the antenna before and after the installation of the new feed cone. Slight changes in the elevation dependence of the aperture efficiency have been detected and the peak antenna gain was measured.

This recalibration of the DSS 13 antenna was conducted to maintain the high precision capability required for performance evaluations of DSN antennas and for radio astronomy research programs. An example of the latter is the Jupiter Patrol (Ref. 2), by which variations in the radio emission from the Jovian radiation belts have been successfully monitored for the past decade. The one-sigma precision of Jupiter's flux-density measurements has been ±2% (±0.1 dB). The effective gain of the antenna near the elevation of transit for the ISEE-3 spacecraft was also determined, and these results were used to evaluate carrier power measurements from the spacecraft.

II. Observations

A selected list of five calibration sources were observed for several hours on January 26, January 29, and February 16, 1982. The observing sessions were planned so that the sources could be measured over a wide range of elevation angles. The intensity of each source was measured several times each night using the drift-curve technique described in Ref. 2.

The one-sigma uncertainty of each source-temperature measurement was less than ±0.1 dB. To achieve this precision, corrections were applied to account for residual pointing errors and a noise-adding radiometer (NAR) subsystem was used to provide receiver gain stabilization. The feed subsystem was switched to the low-noise listen-only configuration (Ref. 1) to optimize the system sensitivity.

The absolute calibration is determined by the flux density scale published by Baars et al. (Ref. 4). This work is widely

used by the radio astronomy community. The primary reference source is Virgo A (3C274), which unfortunately was not visible during the available observing time. However, the flux densities of the five sources that were observed were calculated from the previously observed ratios of their intensities relative to Virgo A (Refs. 3 and 5).

The flux density adapted for Virgo A at 2295 MHz is 140.0 Jy. The flux densities of Virgo A and the calibration sources were calculated at 2270 MHz from the fluxes at 2295 MHz and the spectral indices given in Ref. 4.

The source list and the flux densities used at both frequencies are given in Table 1. The number, N, of independent measurements is given in the third column. The correction factor C_R, listed in the fifth column, is applied to the measurements to account for the loss of intensity due to the angular resolution of the antenna beam, which partially resolves the spatial structure of some radio sources. The effect is small, but not negligible, for the sources included in this report. The source temperatures and the effective aperture efficiency η are discussed below.

III. Effective Aperture Efficiency

The effective aperture efficiency is equal to the ratio of the observed source temperature and the theoretical source temperature for a 100% efficient antenna, $T(\eta = 100\%)$. The latter is given by the expression:

$$T(\eta = 100\%) = \frac{\pi D^2}{4} \frac{S}{2k} \frac{1}{C_R}, \text{ kelvin} \qquad (1)$$

where D is the antenna diameter, S is the flux density of the source, $k = 1.3806 \times 10^{-23}\ Ws^{-1}\ K^{-1}$ is the Boltzmann constant and C_R is the resolution correction factor. For D = 25.91 m (85.0 ft) and flux density S expressed in Jy (1 Jy = 10^{-26} Wm^{-2} Hz^{-1})

$$T(\eta = 100\%) = 0.19095 \frac{S}{C_R}, \text{ kelvin} \qquad (2)$$

The values of $T(\eta = 100\%)$ are given in the 6th column of the table, adjacent to the observed source temperatures. The calculated effective aperture efficiencies are given in the last column. The weighted averages of η for the two frequencies are also given beneath the entries in the last column. The weighted average of the effective aperture efficiency for all seven entries is 0.594 ± 0.002. The uncertainty is the one-sigma standard error calculated from the scatter in the measurements.

The measured efficiency is the effective aperture efficiency because the data are affected by systematic attenuation in the clear atmosphere as well as certain losses in the feed system. With the NAR, all system temperatures are calibrated with respect to the temperature of the NAR reference diode, which is injected into the system via a waveguide coupler at the input to the maser. Consequently, the radio source temperatures are referenced to the waveguide flange at the maser input.

IV. Elevation Dependence of Aperture Efficiency and Gain

A. Experimental Results

The individual data that resulted in the average results given in Table 1 are plotted in Fig. 1 as a function of source elevation angle. The curve represents an empirically determined function of the elevation dependence. The equation is given by:

$$\eta(El) = \eta(37^\circ) A e^{-\tau \sec Z} [(1 - a) + a \cos(El - 30^\circ)] \qquad (3)$$

where $\eta(El)$ is the effective aperture efficiency at elevation El, A is a normalization factor, $\tau = 0.007$ is the atmospheric loss factor at S-band frequencies, Z is the zenith angle of the source ($Z = 90^\circ - El$). Note that τ is the atmospheric attenuation in nepers at zenith and that 1 neper ≃ 4.343 dB. The coefficient $a = 0.098$ was empirically determined from the data in Fig. 1.

Written in this form, Eq. (3) is the expression for the elevation dependence of the effective efficiency as observed by an experimenter. The equation is normalized to $El = 37^\circ$ to match the observed peak in the efficiency measurements. The factor $A = 1.0110$ normalizes the curve to unity at $El = 37^\circ$. The last factor $[(1 - a) + a \cos(El - 30^\circ)]$ represents the loss in efficiency due to gravity loading. The measured symmetry about $El = 30^\circ$ suggests that the peak efficiency of the antenna should occur near 30° elevation when atmospheric losses are removed.

The average values of the effective aperture efficiency for each source (Table 1) are the average values of $\eta(37^\circ)$, which were found by solving Eq. (3) for each measurement. The effective aperture efficiency was converted to antenna gain for a frequency of 2295 MHz. The equivalent antenna gain scale (in dB) is plotted along the right-hand ordinate. Using this scale one can see in Fig. 1 that the peak antenna gain, in the presence of atmospheric attenuation, occurs near 37° elevation. The maximum value of the antenna gain, referred to the reference flange at the input to the maser, is 53.65 ±

0.16 dB at 2295 MHz. The corresponding peak gain at 2270 MHz, not shown in the figure, is 53.56 ± 0.16 dB.

The uncertainties quoted for the peak gain results are the one-sigma error estimates for the two frequencies. The error budget includes the standard error on the measured values of η (±1%), the absolute uncertainty of the flux-density calibration scale (±3%), and the systematic error of the NAR temperature calibration (±2.0%). If these errors are uncorrelated, the resultant error is ±3.7%, or ±0.16 dB. The peak effective aperture efficiency, with its total one-sigma error estimate, is $\eta(37^\circ) = 0.594 \pm 0.022$.

B. Comparison with Calculated Predictions

In order to compare the effective aperture efficiency reported in this article with efficiency calculations performed for the S-X common aperture feed, corrections must be applied to account for attenuation through the clear atmosphere at Goldstone and for attenuation between the input flange of the maser and the aperture of the feed. The first step is to write Eq. (3) for $El = 30^\circ$ (the peak in the antenna gain curve without atmospheric losses):

$$\eta(30^\circ) = \eta(37^\circ) A e^{-\tau \sec(90^\circ - 30^\circ)} \quad (4)$$

Next, multiply by $e^{+\tau \sec(90^\circ - 30^\circ)}$ to remove atmospheric attenuation and divide by f_L (the waveguide loss factor)

$$\eta^*(30^\circ) = (A/f_L)\eta(37^\circ) \quad (5)$$

where $\eta^*(30)$ is the maximum aperture efficiency for this antenna referred to the phase center of the common aperture feed. From J. Withington (private communication) $f_L = 0.98 \pm 0.002$ (-0.09 dB) is the loss factor in the waveguide that includes two switches, three bends, and a rejection filter at the X-band transmitter fundamental frequency. With $A = 1.0110$, the solution to Eq. (5) is

$$\eta^*(30^\circ) = 1.0316\,\eta(37^\circ) = 0.613 \pm 0.022 \quad (6)$$

$\eta^*(30)$ can be compared with calculations of the overall aperture efficiency for this feed, prepared by Williams and Reilly (Ref. 6). Their result is 0.578.

A review (private communication, D. A. Bathker) of the predicted aperture efficiency has been done. Three factors have been identified as principal sources of uncertainty in the predictions. The largest uncertainty is the spar (or quadripod) blockage, which was assumed to consist of the optical shadow area inflated by a factor of 1.2 to account for diffraction at S-band wavelengths. A likely 3σ tolerance on the 0.861 spar blockage factor used in the predictions is $^{+0.04}_{-0.00}$. The next largest uncertainty is the forward spillover for this dual-band feed, which is higher than older designs at 11.1%. A likely 3σ tolerance on this prediction is $^{+0.02}_{-0.00}$.

Finally, the predictions accepted an estimate of 1.5 mm (0.06 in.) rms for the surface tolerance of both reflectors. This is conservative, and results in a prediction of 0.979 surface efficiency; a likely 3σ tolerance is $^{+0.01}_{-0.00}$. The net (conservative) 3σ tolerance on the overall predicted efficiency is thus $^{+0.07}_{-0.00}$; the one-sigma tolerance is $^{+0.023}_{-0.000}$.

The results of the measurements reported here and the predicted values discussed above are summarized in Table 2. The ratio of the measured and predicted values of antenna-design aperture efficiency at S-band is (0.613/0.578) = 1.0606. The measured efficiency is 6.1% (0.25 dB) greater than that predicted from component evaluation calculations. Although this difference is not statistically significant when the one-sigma error estimates are considered, the difference may be large enough to warrant additional investigation.

V. Discussion and Conclusions

The elevation dependence of the S-band aperture efficiency and the peak gain of the DSS 13 antenna appear to have changed only slightly with the installation of the S-X common aperture feed. The peak efficiency now occurs near 37° elevation, where the effective efficiency is 59.4%. Similar calibration data taken on several occasions between 1972 and 1979 yielded curves with maxima near 50° elevation and peak effective efficiencies of 60.5%. Independent measurements by Freiley, Batelaan, and Bathker (Ref. 5) gave consistent results with a peak effective efficiency of 60.6%.

The shift in the efficiency curve toward lower elevation angles is probably caused by a slight change in focus. The Z-axis subreflector focus was measured soon after the new feed was installed. A proper S-band focus was found when the Z-axis readout, which is a relative measure of distance between the subreflector and the feed, was set at 350 (arbitrary units). The previous value of the S-band focus was 330.

Acknowledgments

I would like to thank D. A. Bathker, C. T. Stelzried, W. F. Williams, and J. R. Withington for reviewing this article and for contributing helpful suggestions and insights. I also thank T. J. Thompson for assistance in processing the data.

References

1. Withington, J. R., and Williams, W. F., "A Common-Aperture S- and X-Band Four-Function Feed Cone," *Proc 1981 Antenna Applications Symposium*, University of Illinois, Sept. 23-25, 1981.

2. Klein, M. J., "The Variability of the Total Flux Density and Polarization of Jupiter's Decimetric Radio Emission," *J. Geophys. Res.*, Vol. 81, pp. 3380-3382, July 1976.

3. Klein, M. J., and Stelzreid, C. T., "Calibration Radio Sources for Radio Astronomy: Precision Flux-Density Measurements at 2295 MHz," *Astron. J.*, Vol. 81 pp. 1078-1083, Dec. 1976.

4. Baars, J. W. M., Genzel, R., Pauliny-Toth, I. I. K., and Witzel, A., "The Absolute Spectrum of Cas A; An Accurate Flux Density Scale and a Set of Secondary Calibrators," *Astron. Astrophys.*, Vol. 61, pp. 99-106, 1977.

5. Freiley, A. J., Batelaan, P. D., and Bathker, D. A., *Absolute Flux Density Calibrations of Radio Sources: 2.3 GHz*, Technical Memorandum 33-806, Jet Propulsion Laboratory, Pasadena, Calif., 1977.

6. Williams, W., and Reilly, H., "A Prototype DSN S/X-Band Feed: DSS 13 Application Status (Fourth Report)," *TDA Progress Report 42-60*, pp. 77-88, Jet Propulsion Laboratory, Pasadena, Calif., Dec. 15, 1980.

Table 1. DSS 13 antenna aperture efficiency, common aperture feed: 1982 January and February data (calibrated with noise adding radiometer)

Source designation (IAU)	Source designation (Other)	N	Flux density, Jy	C_R (26-m ant)	Source temperature, T(η = 100%), K	Source temperature, T(observed), K	η (El = 37°)
				2295 MHz			
0433 + 295	3C123	10	31.94	1.000	6.10	3.61 ±0.01	0.592
1648 + 05	3C348	8	28.10	1.006	5.33	3.22 ±0.02	0.604
1957 + 40	Cygnus A	19	915.00	1.009	173.20	103.30 ±0.02	0.596
							(0.597) ±0.003
				2270 MHz			
0433 + 295	3C123	2	32.24	1.000	6.6	3.61 ±0.17	0.586
0134 + 329	3C48	3	10.80	1.000	2.06	1.23 ±0.06	0.596
1717 − 00	3C353	2	40.64	1.010	7.68	4.50 ±0.06	0.586
1957 + 40	Cygnus A	6	927.50	1.009	175.00	105.00 ±0.40	0.598
							(0.592) ±0.004

Table 2. DSS 13 aperture efficiency S-band results with S-X common aperture feed

Aperture efficiency type	Peak efficiency (±1σ)	Elevation of peak	Reference plane	Notes
Effective; measured	$\eta = 0.594 \pm 0.022$	37°	Maser input	User effective aperture: includes atmospheric and waveguide losses
Antenna design; inferred from measurements	$\eta^* = 0.613 \pm 0.022$	30°	Phase center of feed	Does not include atmospheric or waveguide losses
Antenna design; predicted[1]	$\eta^* = 0.578\ ^{+0.023}_{-0.000}$	–	Phase center of feed	Does not include atmospheric or waveguide losses

[1]Includes feed pattern integration, subreflector and spar blockage, and surface roughness (Ref. 6, and D. A. Bathker, private communication).

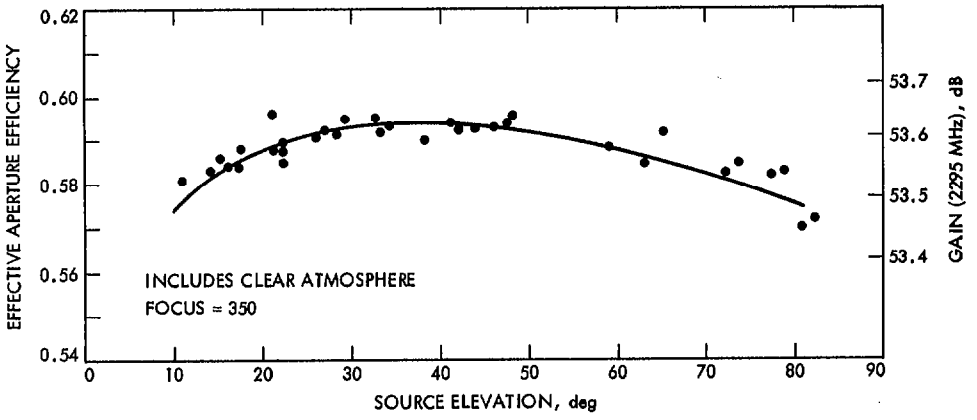

Fig. 1. Elevation dependence of aperture efficiency of the DSS 13 26-m antenna, with S-X common aperture feed, 2295 MHz (1982 January and February data)